

V.V. Turov<sup>1</sup>, V.M. Gun'ko<sup>1</sup>, T.V. Krupskaya<sup>1</sup>, L.S. Andriyko<sup>1</sup>, A.I. Marynin<sup>2</sup>, V.N. Pasichnyi<sup>2</sup>

## THIXOTROPIC SYSTEM BASED ON MIXTURE OF HYDROPHILIC AND HYDROPHOBIC SILICA

<sup>1</sup> *Chuiko Institute of Surface Chemistry of National Academy of Sciences of Ukraine  
17 General Naumov Str., Kyiv, 03164, Ukraine, E-mail: krupska@ukr.net*

<sup>2</sup> *National University of Food Technology  
68 Volodymyrska Str., Kyiv, 01033, Ukraine*

Particles of hydrophilic (A-300) and hydrophobic (AM1) silicas, interacting with each other, form secondary structures in which the gaps between non-porous nanoparticles shape texture mesopores and macropores. Water addition to this system during the process of mechanochemical action results in a forming of composite system with thixotropic properties. Thus, the aim of the work was to study the phase state and parameters of the water binding to the surface of solid particles in systems consisting of two parts of hydrophilic and one part of hydrophobic silica with a variable water content. Using the methods of <sup>1</sup>H NMR spectroscopy, electron microscopy, laser correlation spectroscopy and rheological studies, the state of water was studied, its thermodynamic parameters, as well as the A-300/AM1 composite particle size distribution were determined. It has been found that water in the interparticle gaps of the A-300/AM1 composite is in the form of polyassociates similar to clusters and domains in liquid water. It was shown that with increasing water concentration (from 1 to 4 g/g) in the composite, its bulk density, the amount of strongly bound water and the total change in its free energy increased. It has been found that for composites with different hydration, similar clusters size distributions of adsorbed water are observed, where two maxima are identified at  $R = 5-7$  and  $20-30$  nm, and most of the water is part of cluster structures with radius of  $20-40$  nm. It has been shown that a suspension based on of a mixture of 2/1 hydrophilic and hydrophobic silicas and 3 g/g of water, depending on the mechanical loading, can be in the state of a wet powder or viscous liquid, having high thixotropic properties, which are manifested in diluted aqueous suspensions. For dispersing of such a composite in an aqueous medium, aggregates form in with a diameter of  $80-100$  and  $200-1000$  nm, which indicates intense interparticle interactions. The interaction energy of the nanoparticles surface in the composite with the aqueous medium increases from 12 to 18 J/g with an increase in the water content from 1 to 4 g/g. Under the influence of shear load, the viscosity of the diluted suspension decreases by an order of magnitude, and then is restored at a level which exceeds the initial one almost at twice. It has been found that the obtained colloidal system is irreversible in the aqueous medium and under the mechanical load influence in the working cylinder of a viscometer, its viscosity characteristics intensify.

**Keywords:** thixotropic phenomena, methyl silica, hydrophilic silica, bound water, <sup>1</sup>H NMR spectroscopy

### INTRODUCTION

Pyrogenic silicas are environmentally-friendly materials in which the content of the main substance exceeds 99 %. Biological inactivity and high specific surface area make it possible to use them widely as an effective adsorbent approved for application in medicine for detoxifying both of human and animal organism [1-3], structure-forming filler for many pharmaceutical preparations [4] and a food supplement that improves the technological properties of some products [5]. The creation of new types of functionalized materials for biomedical purposes can be expected in the development of composite systems, which simultaneously include hydrophilic and hydrophobic highly dispersed materials, as well

as organic substances of various chemical nature, giving them the necessary properties [6-9].

The synthesis of hydrophobic methyl silica is carried out by replacing all or most of the surface hydroxyl groups with methylsilyl ones [10, 11]. The initial methyl silicas are not wetted with water, since the interparticle gaps in aggregates ( $<1 \mu\text{m}$ ) of non-porous nanoparticles (NPNP, diameter is about 10 nm), agglomerates of aggregates ( $>1 \mu\text{m}$ ), and visible loose particles (bulk density  $\rho_b \approx 0.05 \text{ g/cm}^3$ ) are filled with air and the water adsorption is thermodynamically unfavorable. However, in works [6-16] it was found that a mixture of hydrophobic oxides (or their mixtures with hydrophilic nano-oxides) with water can be homogenized by grinding using relatively small

mechanical loads, which allows air to be removed from the gaps between the NPNPs in the compacted material ( $\rho_b$  increases by about a magnitude order), replacing it with water. Hydro-compacted nano-oxide, initially hydrophobic, is wettable with water and can form a stable aqueous suspension. However, if this compacted nanooxide is dried, then it regains its hydrophobic properties (for example, the powder will float on the water surface).

The phase state of aqueous suspensions of compacted hydrophobic powders depends on many factors: the solid phase concentration, the concentrations ratio of the hydrophobic and hydrophilic components, the features of the preliminary treatment of oxides, temperature, diffusion of solvents and residual gases, *etc.* In complex heterogeneous systems, the adsorption and technological characteristics of composites largely depend on the processes occurring during their formation, on the creation of supramolecular structures with a minimum free energy. Several types of interactions are typical for aqueous suspensions of such systems: a liquid medium with solid particles, solid nanoparticles with each other, and gaseous substances (air) with solid (primarily hydrophobic) particles [17–19], that are due to van der Waals and electrostatic, dispersion and ionic interactions. As a result, colloidal systems with thixotropic properties can form [20–22]. If in liquids, because of intense molecular movements, thermodynamic equilibrium is set spontaneously (micellar colloids), then in mixtures of nanoscaled solids with various hydrophobic-hydrophilic properties, external influences may be required to achieve thermodynamic equilibrium, in particular, mixing with mechanical load. By adding hydrophobic substances to hydrophilic systems and dosed mechanical action on a multicomponent system in the water presence, new methods can be developed to control the properties of composite systems and the processes of water clustering or aqueous solutions at the interfaces.

Thus, the aim of the work was to study the phase state and parameters of the water binding to the surface of solid particles in systems consisting of two parts of hydrophilic and one part of hydrophobic silica with a variable water content.

## EXPERIMENTAL PART

For experiments, pyrogenic silica A-300 was used and its methylated analogue AM1, obtained as a result of the reaction of dimethyldichlorosilane with A-300 (Pilot plant of Chuiko Institute of Surface Chemistry, Kalush, Ukraine). The bulk density of both silicas was 0.045–0.05 g/cm<sup>3</sup>. To prepare the composite system, the selected amounts of silica were ground in a porcelain mortar for 10 min. Then the required amount of water was added to the composite and grinding continued until a homogeneous powder or gel-like paste was formed.

The <sup>1</sup>H NMR spectra were recorded using a Varian 400 Mercury spectrometer of high resolution with an operating frequency of 400 MHz. Eight probing 60° impulses of 1 μs duration were used with a bandwidth of 20 kHz. The temperature was controlled by means of a Bruker VT-1000 device with an accuracy of ±1 deg. The signal intensities were determined by measuring the area of the peaks using the procedure for decomposing the signal into its components under the assumption of a Gaussian form of signal and optimizing of the zero line and phase with an accuracy that was not less than 5% for well-resolved signals and ±10 % for overlapping signals. To prevent supercooling of the studied systems, the measurements of the amounts of unfrozen water (at  $T < 273$  K) were carried out on heating of samples preliminarily cooled to 210 K. The temperature dependences of the <sup>1</sup>H NMR signals intensity were recorded in an automated cycle, when the holding time of the sample at a certain constant temperature was 9 min, and the measurement time was 1 min. NMR measurements were carried out in the air medium.

The rheological properties of the dispersions were studied using a rotational viscometer “Rheotest 2.1” (cylinder system S/N) at a shear rate of 9–1312.2 s<sup>-1</sup>. The relative measurement error was  $\delta_I = \pm 4$  %.

Particle size distribution investigations for the nanosilica dispersion was carried out using a Zetasizer Nano ZS (Malvern Instruments) apparatus with a universal dip cell (ZEN1002).

## RESULTS AND DISCUSSION

TEM micrographs of the composite system obtained by grinding 2 parts of hydrophilic silica

A-300 and 1 part of hydrophobic silica AM1 (before water addition) are shown in Fig. 1. Secondary structures are observed in the composite, having the size of several microns. With an increase in resolution, primary silica particles with a size of 10–20 nm become visible. These particles interacting with each other, create secondary structures, where the

gaps between NPNPs form textural mesopores (with a radius of  $1 \text{ nm} < R < 25 \text{ nm}$ ) and macropores ( $R > 25 \text{ nm}$ ) with an insignificant contribution of micropores ( $R < 1 \text{ nm}$ ). The hydrophilic and hydrophobic components do not differ in micrographs, since hydrophilic A-300 was as the basis for the hydrophobic AM1 synthesis.

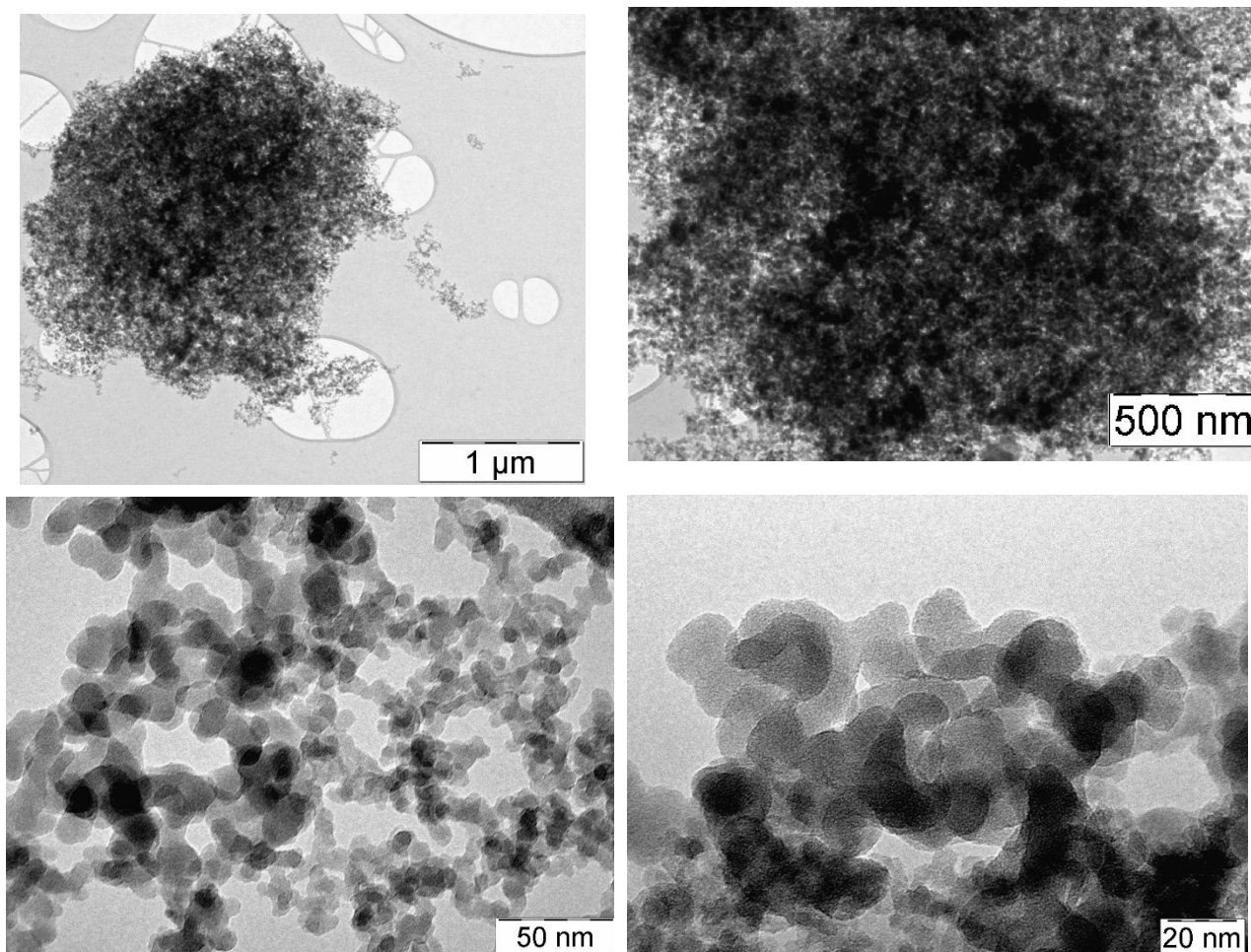


**Fig. 1.** TEM images of composite system containing hydrophilic A-300 and hydrophobic AM-1 silicas in the ratio (2/1)

The  $^1\text{H}$  NMR spectra of water bound in a composite system consisting of hydrophilic and hydrophobic silicas taken at different temperatures in the water concentration range  $h = 1 - 4 \text{ g}$  per gram of dry substance are shown in Fig. 2 *a-d*, and in Fig. 2 *e* – for a sample containing  $4 \text{ g/g}$   $\text{H}_2\text{O}$  in deuteriochloroform medium. In the spectra single water signal is observed with chemical shift ( $\delta_H$ ) is about 4.5 ppm at  $T = 283 \text{ K}$ . The signal intensity reduces with decreasing temperature in accordance with the freezing of a part of the

adsorbed water, but the chemical shift increases (Fig. 3).

The value of the water chemical shift (i.e., the average value of the trace of the magnetic shielding tensor of protons in water molecules relative to the standard – tetramethylsilane) localized in the NPNPs interparticle gaps in silica is determined by the average number of hydrogen bonds in which each water molecule participates, the strength of hydrogen bonds, and the presence in the subsurface layer of hydrated structures with an excess charge (for example,

solvated protons or other ions). Chemical shift of non-associated water (gaseous state or non-polar medium)  $\delta_H = 1 - 1.5$  ppm [23, 24], for tetracoordinated water in ice –  $\delta_H = 7$  ppm [25], for liquid water, depending on temperature, intermediate values  $\delta_H = 4 - 6$  ppm are characteristic, which correspond to the participation of each molecule in 2–3 hydrogen bonds with its neighbors. In solutions, the chemical shift value is also determined by the statistical contribution from the solvate – solvant associates [26–28].

According to the data in Figs. 2, 3, water in the interparticle gaps of the A-300/AM1 composite is in the form of some polyassociates, similar to clusters and domains in liquid water [29–31]. With temperature decreasing, molecular

mobility reduces, and the molecules ordering increases. In some cases, on the surface the structures are formed, characterizing by a high value of the chemical shift, up to  $\delta_H = 8.5$  ppm. Probably, a certain number of associates containing solvated protons are present on the surface, the chemical shift of which can be  $\delta_H = 12$  ppm [32]. The chloroform medium has a little effect on the chemical shift of adsorbed water. This indicates that chloroform does not displace water in contact with the surface [33], since under conditions of complete filling of the interparticle gaps of composite particles with water, diffusion of weakly polar molecules can proceed rather slowly. In addition, this process can be energetically unfavorable due to the need to change the structure of aggregates.

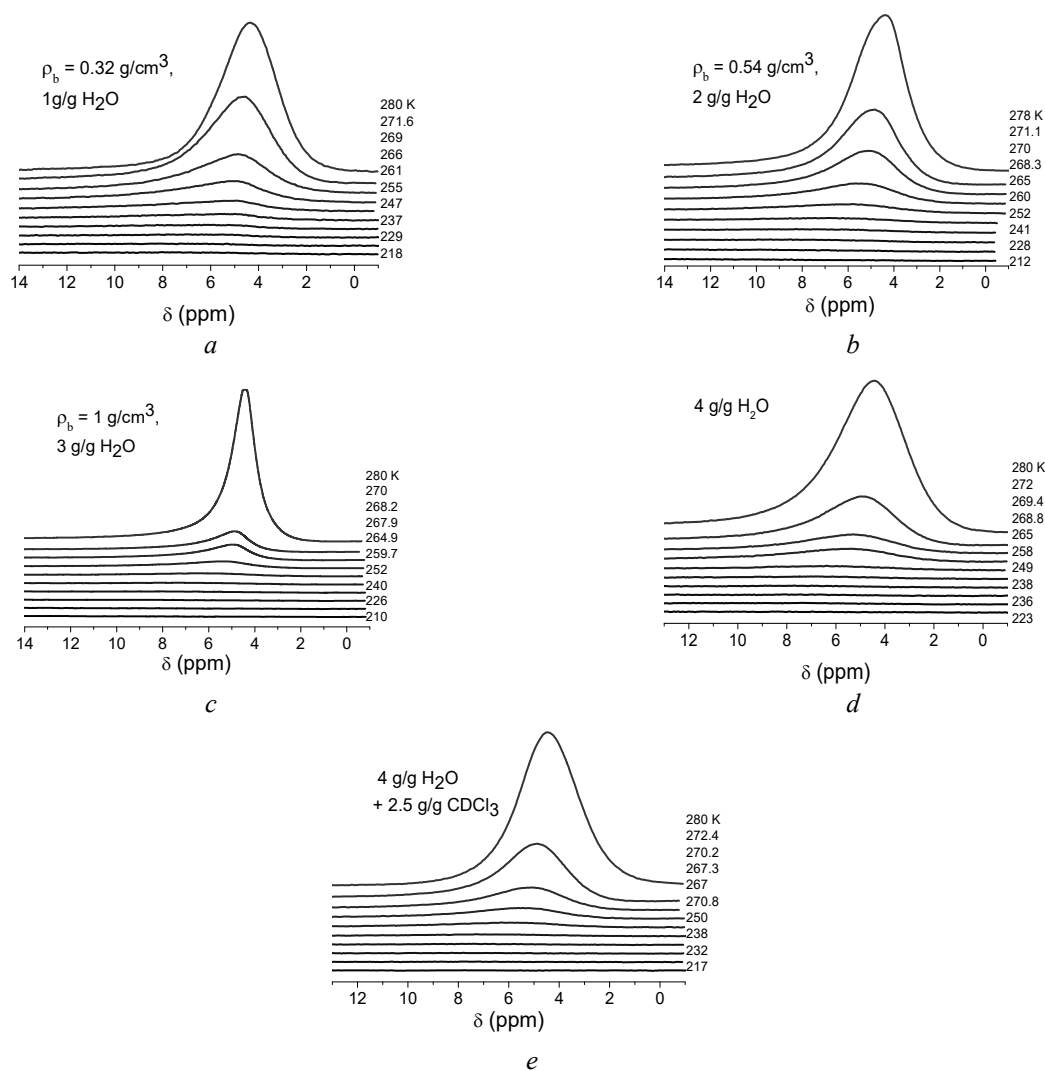


**Fig. 2.**  $^1\text{H}$  NMR spectra (recorded at different temperatures) of water adsorbed by the composite system A-300/AM-1 (2/1), at  $h = 1 - 4 \text{ g/g}$  (a–d, respectively) and at  $h = 4 \text{ g/g}$  in  $\text{CDCl}_3$  medium (e)

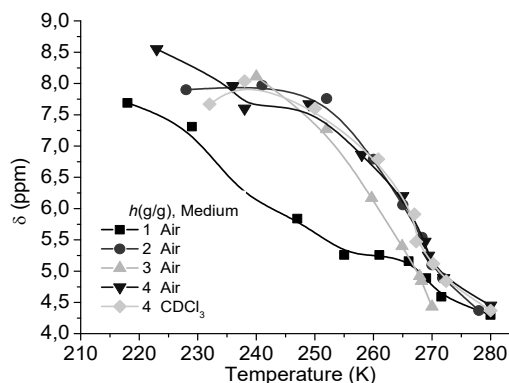


**Fig. 3.** Temperature dependences of the chemical shift of water adsorbed in the interparticle gaps of the composite system A-300/AM-1 at different hydration degree

Since the water concentration in the samples is known, the intensity of the water signal ( $I$ ) can be used to calculate the concentration of unfrozen water ( $C_{uw}$ ) at any temperature:  $C_{uw} = hI_T/I_{T>273}$ . The corresponding dependences for composite systems A-300/AM1, differing in water content, are shown in Fig. 4 *a*. The process of freezing (melting) of interfacial water, localized in a solid porous matrix, takes place in accordance with changes in the Gibbs free energy due to the influence of the surface. The farther the studying layer of water is from the surface, the less the influence is at  $T = 273$  K water freezes, the properties of which do not differ from those of bulk water, and as the temperature decreasing (without taking into account the effect of supercooling), the water layers, that are located closer to the surface, freeze. Thus, for interface water the ratio is valid:

$$\Delta G_{ice} = -0.036(273.15 - T), \quad (1)$$

where the numerical coefficient is a parameter, associated with the temperature coefficient of variation of the Gibbs free energy for ice [34]. Determining the concentration of unfrozen water as a function of temperature  $C_{uw}(T)$  by the signal intensity, in accordance with the technique detailed in [33, 35–37], the amount of strongly and weakly bound water (SBW and WBW, respectively) and the thermodynamic characteristics of these layers can be calculated. [34]. Fig. 4 shows the temperature dependences of the concentration of unfrozen water (Fig. 4 *a*) and the dependences of the change in the Gibbs free energy on the concentration of unfrozen water  $\Delta G(C_{uw})$  calculated on their basis (Fig. 4 *b*).

If the total water content in the system significantly exceeds the total pore volume (interparticle gaps), then some part of the water can be in a free (unbound) state when water molecules do not experience a disturbing effect from the particle surface. It is difficult to determine accurately the amount of “bulk” water, therefore, we will consider that part of water that corresponds to  $h > 1.5$  g/g as bulk one.

The interfacial energy of solids or biopolymers was determined as a modulus of the total decrease in the free energy of absorbed water, due to the presence of an internal water-polymer interface by the formula,

$$\gamma_s = -K \int_0^{C_{uw}^{\max}} \Delta G(C_{uw}) dC_{uw}, \quad (2)$$

where  $C_{uw}^{\max} = 1.5$  g/g.

Interfacial energy is a convenient parameter that allows you to compare the energy of water binding in different systems, especially if the amount of water in them is the same.

To determine the geometrical dimensions of nanoscale aggregates of liquid limited by solid surface, the Gibbs – Thomson equation [38, 39] can be used, connecting radius of spherical or cylindrical pores ( $R$ ) with the value of the depression of freezing temperature:

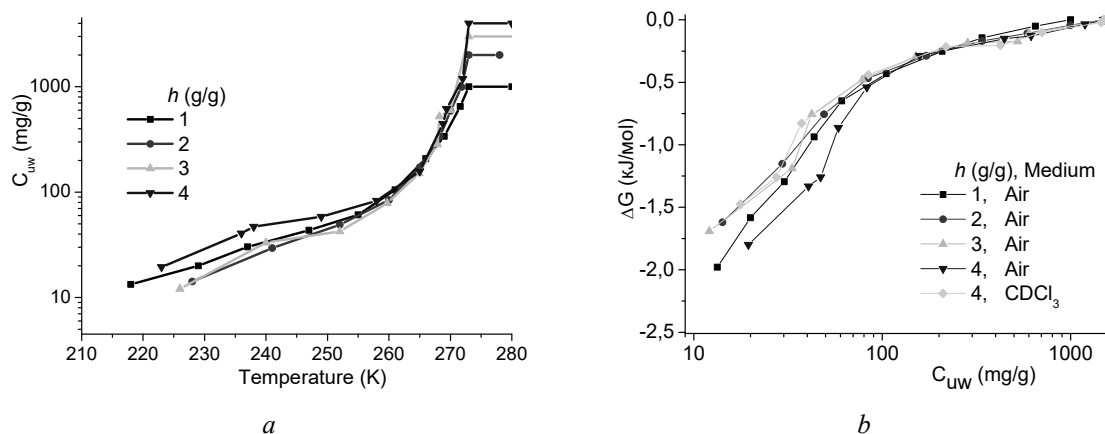
$$\Delta T_m = T_m(R) - T_{m,\infty} = \frac{2\sigma_{sl}T_{m,\infty}}{\Delta H_f \rho R} \quad (3)$$

where  $T_m(R)$  is melting temperature of ice in the pores (voids) of radius  $R$ ,  $T_{m,\infty}$  – bulk melting temperature of ice,  $\rho$  – density of the solid phase,  $\sigma_{sl}$  – the energy of the solid-liquid interaction

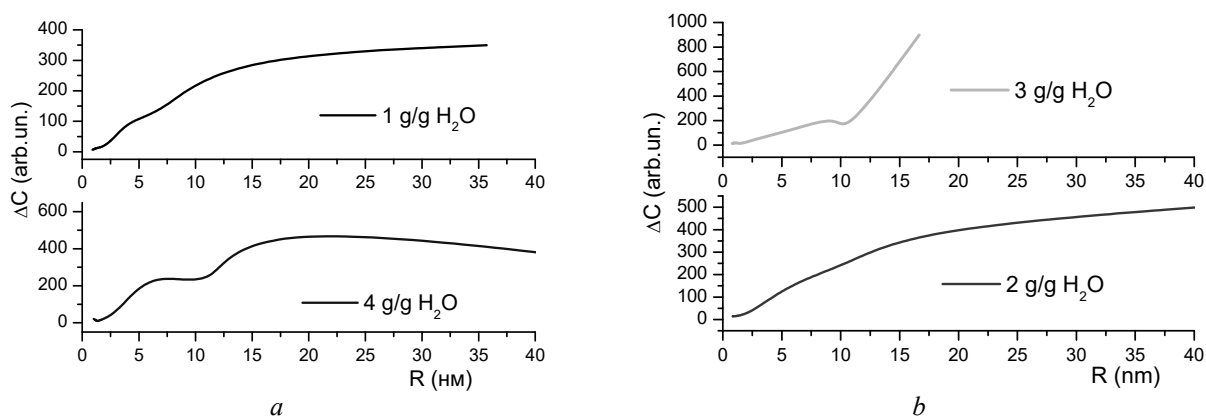
(for example, via hydrogen bonds),  $\Delta H_f$  – the bulk enthalpy of melting.

Table demonstrates the characteristics of unfrozen water layers in the composite system A-300/AM-1 (2/1) with different hydration. Wherein the concentration of strongly and weakly bound water ( $C_{uwS}$  and  $C_{uwW}$ , respectively), and maximum reduction of Gibbs energy in a layer of strongly bound water ( $\Delta G_S$ ) were calculated, that was estimated by extrapolating the dependence  $\Delta G(T)(C_{uw})$  to the

ordinate axis ( $\Delta G$ ), as well as the surface energy value calculated in accordance with the formula (2). Strongly bound was considered to be a part of the interfacial water for which the decrease in the Gibbs free energy of  $\Delta G < -0.5$  kJ/mol [34–36]. Size distributions of adsorbed water clusters were calculated according to the formula (3). For clarity, they are shown in Fig. 5 together with the dependence  $\gamma_s(h)$ . Bulk density could be determined only for samples at  $h \leq 3$  g/g.



**Fig. 4.** Dependences of the change in the unfrozen water concentration on temperature (a) and constructed on their basis the dependences of the change in the Gibbs free energy on the unfrozen water concentration (b) in the interparticle gaps of the composite system A-300/AM-1 at different hydration



**Fig. 5.** Size distribution of adsorbed water clusters at different hydration of A-300/AM-1 (2/1)

Assuming that the bound water in composites can be no more than 1.5 g/g, and strongly bound is the part for which  $\Delta G \leq -0.5$  kJ/mol, then we can calculate the parameters of the unfrozen water layers, including the specific surface area of oxides in contact with it and the volume of pores filled

with unfrozen water, as well as the average melting temperature of ice (Table). As the water concentration rises in the composite, its bulk density, the amount of strongly bound water, and the total change in its free energy enhance. The  $\gamma_s$  dependence monotonically increases over the entire range of changes in hydration (Table). A

fourfold rise in the adsorbed water amount leads to a relatively small (up to 30 %) increase in the interfacial energy: in the range  $1 < h < 4$  g/g addition of new portions of water does not result in a noticeable enhance in its binding to the surface of composite particles. A possible reason should be considered the limited volume of pores and the accessible particles surface in the compacted system and the weak surface effect on remote water layers. Inclusion in the sample with  $h = 4$  g/g H<sub>2</sub>O 2.5 g/g deuteriochloroform leads only to a slight decrease in the interfacial energy (Table) due to a reduce in the amount of strongly bound water, which indicates the possibility of partial displacement of bound water by chloroform.

For the composites with different hydration degree, similar in form of size distributions of adsorbed water clusters are observed (Fig. 5). Two maxima are identified on them at  $R = 5-7$

and 20–30 nm. Most part of the water is included in the composition of cluster structures with the radius of 20–40 nm, with the exception of a sample containing 3 g/g of adsorbed water, for which it was not possible to measure the intensity of its signal near  $T = 273$  K (Fig. 2 c).

In concentrated systems such as studied composites, strong interparticle interactions can exist, the magnitude of which depends on the solid phase concentration. Fig. 6 shows the results of measuring the diameter distributions of the composite particles, taken by the method of laser correlation spectroscopy at diluting of a sample containing 2 parts of hydrophilic, one part of hydrophobic silica and 3 g/g water, up to 5, 1.4, and 0.23 wt% dry substance (samples 1–3) after sonicating for 10 min (samples 2, 3) and 40 min (sample 1). Fig. 6 shows curves for scattered light intensity, volume and number of particles vs particle diameter.

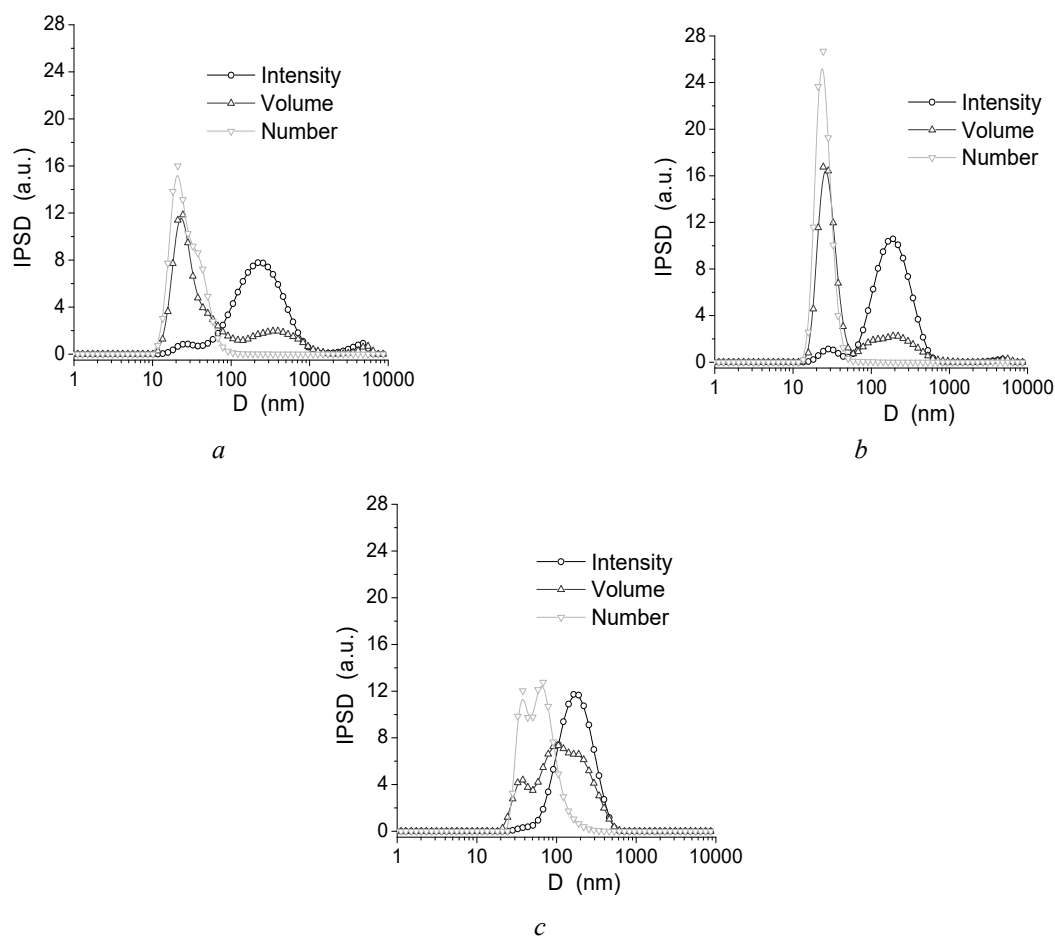


**Fig. 6.** Particle size distribution of aqueous suspension A-300/AM-1 (2/1) composite at different concentration of dry substance: *a* – 5, *b* – 1.4, *c* – 0.23 wt. %

**Table 1.** Characteristics of unfrozen water layers in the composite system A-300/AM-1 (2/1) at different hydration

$h$ , g/g	$\rho_b$ , g/cm <sup>3</sup>	Medium	$C_{uw}^s$ , mg/g	$C_{uw}^w$ , mg/g	$-\Delta G_s$ , kJ/mol	$\gamma_s$ , J/g	$\langle T_m \rangle$ , K	$S_{nano,uw}$ , m <sup>2</sup> /g	$S_{meso,uw}$ , m <sup>2</sup> /g	$S_{macro,uw}$ , m <sup>2</sup> /g	$V_{nano,uw}$ , cm <sup>3</sup> /g	$V_{meso,uw}$ , cm <sup>3</sup> /g	$V_{macro,uw}$ , cm <sup>3</sup> /g
1.0	0.32	Air	60	940	2.66	12.1	264.3	13	41	5	0.006	0.639	0.355
2.0	0.54	Air	85	1415	2.25	13.8	265.9	0	61	10	0	0.851	1.149
3.0	1.0	Air	75	1425	2.31	17.9	268.3	0	100	18	0	1.819	1.181
4.0	–	Air	98	1402	2.63	18.2	267.2	9	72	28	0.004	1.305	2.691
4.0	–	CDCl <sub>3</sub>	85	1415	2.08	15.0	267.1	0	61	6	0	1.230	2.770



In the most concentrated suspension (sample 1, Fig. 6 *a*), approximately two thirds of the total volume of particles are particles with diameters in the range  $D = 10\text{--}80$  nm, and a third in the range  $D = 200\text{--}1000$  nm. When the suspension is diluted, the volume of large particles slightly decreases (sample 2, Fig. 6 *b*), and in the diluted suspension, three maxima are recorded on the distribution curve at  $D = 30, 100$  and  $300$  nm (Fig. 6 *c*). For suspensions of pyrogenic oxides, the polymodality of particle distributions is a common phenomenon, since NPNPs form hierarchical structures of aggregates and agglomerates, the appearance of which is due to the nature of pyrogenic synthesis and the subsequent history of materials. Whereas a stable highly concentrated suspension

(5.5 wt. %) is formed only in the case of prolonged sonication, it should be concluded that composites prepared on the basis of hydrophilic and hydrophobic silicas mixtures are characterized by strong interparticle interactions, the magnitude of which depends on the method of sample preparation. It turned out that the composite A-300/AM-1 (2/1), prepared at  $h = 3$  g/g, has high thixotropic properties. Immediately after preparation, it has a gel-like appearance. However, after several hours of aging without mechanical stress, it turns into a solid that can be crushed into components and looks like a wet powder (Fig. 7 *a*). This process is reversible, because after light grinding in a porcelain mortar, the powder turns into a viscous liquid again (Fig. 7 *b*).

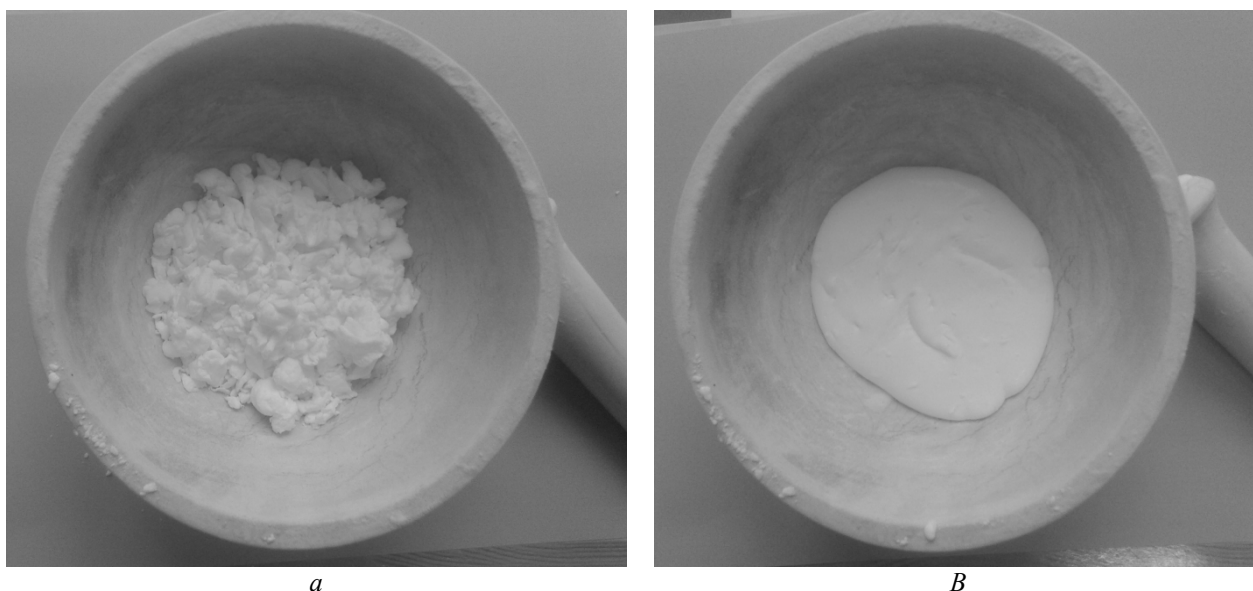


**Fig. 7.** Change in the phase state of the A-300/AM1 (2/1) composite containing 3 g/g H<sub>2</sub>O: initial (*a*) and after slight grinding (*b*)

The thixotropic properties of the system are determined by its capability to change the viscosity depending on the applied shear load [17, 18]. Fig. 8 shows the results of measuring the shear viscosity over time at various shear loads, obtained on a Rheotest 2.1 viscometer using a cylindrical system in the shear rate range from 9 to 1300 s<sup>-1</sup>. The relative measurement error was  $\delta_l = \pm 4\%$ . The measurements were carried out in the mode of stepwise change in shear loads. As the shear load increases, the viscosity of the colloidal system decreases from

90 to 30 mPa·s. Holding the sample for 10 min at a constant shear load does not lead to a change in its viscosity, but the return of the system to a stable state (no load) is accompanied by a noticeable (in comparison with the initial value) increase in viscosity. Thus, a colloidal system based on a mixture of hydrophilic and hydrophobic silicas at the ratio of 2/1 in an aqueous medium is irreversible and under the influence of mechanical stress in the working cylinder of a viscometer, its viscosity characteristics intensify.

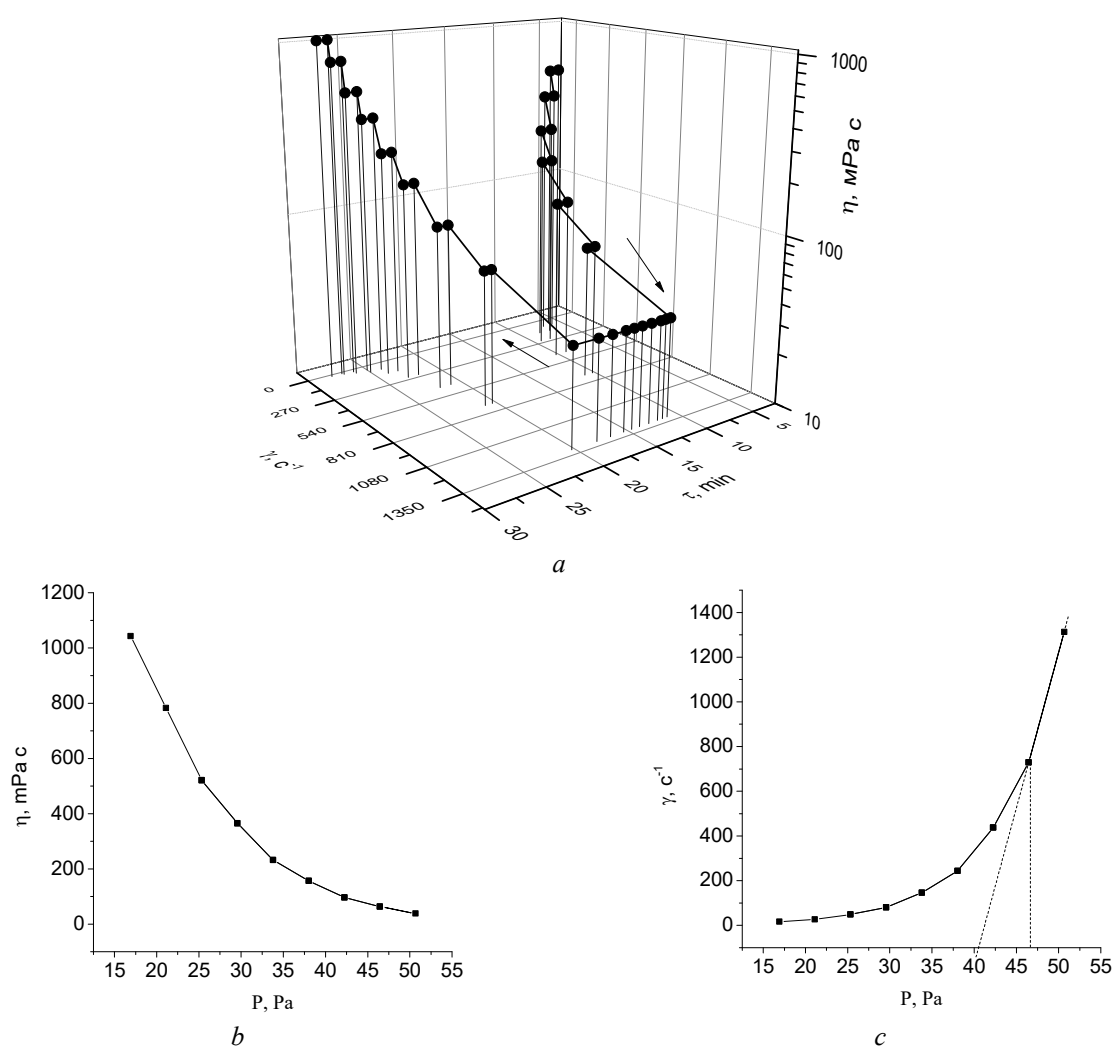


**Fig. 8.** The dependence of viscosity ( $\eta$ , mPa·c) on shear rate ( $\dot{\gamma}$ , c<sup>-1</sup>) in time ( $t$ , min) for (a); effective viscosity ( $\eta$ , mPa·c) on shear stress ( $P$ , Pa) (b) and shear rate ( $\dot{\gamma}$ , c<sup>-1</sup>) on shear stress ( $P$ , Pa) (c)

## CONCLUSIONS

A composite system obtained by grinding 2 parts of A-300 hydrophilic silica and 1 part of AM1 hydrophobic silica forms stable aggregates in which the primary particles have a diameter of about 10–20 nm, and the gaps between nanoparticles form a developed mesoporous structure. Under the influence of mechanical loading, mesopores in a mixture can be filled with water, which is in a clustered state, characterized by the participation of each water molecule in the formation of 2–3 hydrogen bonds. Most of the bound water is included in clusters with a radius not exceeding 40 nm. A suspension prepared on the basis of a mixture of hydrophilic and hydrophobic silicas (2/1) and 3 g/g of water, depending on the mechanical

loading, can be in the state of a wet powder or a viscous liquid, having high thixotropic properties, which are manifested in dilute aqueous suspensions. When dispersed in an aqueous medium, aggregates form with a diameter of 80–100 and 200–1000 nm in such composite. This indicates intense interparticle interactions. In the composite with an aqueous medium, the interaction energy of the nanoparticle surface increases from 12 to 18 J/g with an increase in the water content from 1 to 4 g/g. Under the influence of the shear load, the viscosity of the diluted suspension decreases by a magnitude order and then recovers at a level that is almost two times higher than the initial one.

*The article contains the results of research carried out with grant support under the competitive project of the target program of scientific research of the National Academy of*

*Sciences of Ukraine N 19-20 and the target program of fundamental research of the National Academy of Sciences of Ukraine N 33/20-N.*

## **Тиксотропна система на основі суміші гідрофільного та гідрофобного кремнеземів**

**В.В. Туров, В.М. Гунько, Т.В. Крупська, Л.С. Андрійко, А.І. Маринін, В.М. Пасічний**

*Інститут хімії поверхні ім. О.О. Чуйка Національної академії наук України  
вул. Генерала Наумова, 17, Київ, 03164, Україна, krupskaya@ukr.net  
Національний університет харчових технологій  
вул. Володимирська, 68, Київ, 01033, Україна*

*Частинки гідрофільного (А-300) та гідрофобного (АМ-1) кремнеземів, взаємодіючи між собою, утворюють вторинні структури, в яких проміжки між непористими наночастинками формують текстурні мезо- і макропори. При додаванні до цієї системи води в процесі механохімічної обробки відбувається утворення композитної системи, яка має тиксотропні властивості. Метою роботи було вивчення фазового стану та параметрів зв'язування води з поверхнею твердих частинок в системах, що складаються з двох частин гідрофільного і однієї частини гідрофобного кремнеземів при варіюванні вмісту води. Методами <sup>1</sup>Н ЯМР спектроскопії, електронної мікроскопії, лазерної кореляційної спектроскопії, реологічних досліджень вивчено стан води та визначено її термодинамічні параметри, досліджено розподіл за діаметрами частинок композиту. Встановлено, що вода в міжчастинкових проміжках композиту А-300/АМ1 знаходиться у вигляді поліасоціатів, які є аналогічними кластерам і доменам в рідкій воді. Показано, що при збільшенні концентрації води (від 1 до 4 г/г) в композиті підвищується його насипна густина, кількість сильнозв'язаної води та сумарна зміна її вільної енергії. Визначено, що для композитів з різною гідратацією спостерігаються схожі за виглядом розподіли по радіусах кластерів адсорбованої води, де ідентифікуються два максимуми при R = 5–7 і 20–30 нм, а велика частина води входить до складу кластерних структур, радіус яких становить 20–40 нм. Показано, що суспензія, приготована на основі суміші 2/1 гідрофільного і гідрофобного кремнеземів і 3 г/г води, в залежності від механічного навантаження, може перебувати в стані в'язкої рідини або вологого порошку і має високі тиксотропні властивості, які проявляються в розведених водних суспензіях. При диспергуванні у водному середовищі такий композит формує агрегати діаметром 80–100 і 200–1000 нм, що свідчить про інтенсивні міжчастинкові взаємодії. Енергія взаємодії поверхні наночастинок в композиті з водним середовищем збільшується від 12 до 18 Дж/г із зростанням вмісту води від 1 до 4 г/г. Під впливом навантаження зсуву в'язкість розведеної суспензії зменшується на порядок, а потім відновлюється на рівні, який перевищує вихідний майже в два рази. Встановлено, що отримана колоїдна система в водному середовищі необоротна і під впливом механічного навантаження в робочому циліндрі віскозиметра змінює свої в'язкісні властивості в бік збільшення.*

**Ключові слова:** тиксотропні явища, метилкремнезем, гідрофільний кремнезем, зв'язана вода, <sup>1</sup>Н ЯМР-спектроскопія

## Тиксотропная система на основе смеси гидрофильного и гидрофобного кремнезёмов

В.В. Туров, В.М. Гунько, Т.В. Крупская, Л.С. Андрийко, А.И. Маринин, В.Н. Пасичный

Институт химии поверхности им. А.А. Чуйко Национальной академии наук Украины  
ул. Генерала Наумова, 17, Киев, 03164, Украина, [krupska@ukr.net](mailto:krupska@ukr.net)  
Национальный университет пищевых технологий  
ул. Владимирская, 68, Киев, 01033, Украина

Частицы гидрофильного (А-300) и гидрофобного (АМ-1) кремнезёмов, взаимодействуя между собой, образуют вторичные структуры, в которых зазоры между непористыми наночастицами формируют текстурные мезо- и макропоры. При добавлении к этой системе воды в процессе механохимического воздействия происходит образование композитной системы, которая обладает тиксотропными свойствами. Целью работы было изучение фазового состояния и параметров связывания воды с поверхностью твердых частиц в системах, состоящих из двух частей гидрофильного и одной части гидрофобного кремнезёма при варьируемом содержании воды. Методами <sup>1</sup>H ЯМР спектроскопии, электронной микроскопии, лазерной корреляционной спектроскопии, реологических исследований изучено состояние воды и определены ее термодинамические параметры, исследовано распределение по диаметрам частиц композита. Установлено, что вода в межчастичных зазорах композита А-300/АМ1 находится в виде полиассоциатов, аналогичных кластерам и доменам в жидкой воде. Показано, что с ростом концентрации воды (от 1 до 4 г/г) в композите повышается его насыпная плотность, количество сильносвязанной воды и суммарное изменение ее свободной энергии. Определено, что для композитов с разной гидратацией наблюдаются схожие по виду распределения по радиусам кластеров адсорбированной воды, где идентифицируются два максимума при  $R = 5-7$  и  $20-30$  нм, а большая часть воды входит в состав кластерных структур, радиус которых составляет 20–40 нм. Показано, что суспензия, приготовленная на основе смеси 2/1 гидрофильного и гидрофобного кремнезёмов и 3 г/г воды, в зависимости от механической нагрузки может находиться в состоянии вязкой жидкости или влажного порошка и имеет высокие тиксотропные свойства, проявляющиеся в разбавленных водных суспензиях. При диспергировании в водной среде такой композит формирует агрегаты диаметром 80–100 и 200–1000 нм, что свидетельствует об интенсивных межчастичных взаимодействиях. Энергия взаимодействия поверхности наночастиц в композите с водной средой увеличивается от 12 до 18 Дж/г с ростом содержания воды от 1 до 4 г/г. Под влиянием сдвиговой нагрузки вязкость разбавленной суспензии уменьшается на порядок, а затем восстанавливается на уровне, который превышает исходный почти в два раза. Установлено, что полученная коллоидная система в водной среде необратима и под влиянием механической нагрузки в рабочем цилиндре вискозиметра изменяет свои вязкостные свойства в сторону увеличения.

**Ключевые слова:** тиксотропные явления, метилкремнезём, гидрофильный кремнезём, связанная вода, <sup>1</sup>H ЯМР-спектроскопия

### REFERENCES

1. *Basic characteristics of Aerosil. Technical Bulletin Pigments*. N 11. (Hanau: Degussa AG, 1997).
2. Чуїко А.А. *Medical chemistry and clinical application of silica dioxide*. (Kyiv: Naukova Dumka, 2003). [in Russian].
3. Туров В.В., Герашченко И.И., Крупская Т.В., Суворова Л.А. *Nanochemistry in solving the problems of endo- and exoecology*. (Stavropol: Zebra, 2017). [in Russian].
4. Legrand A.P. *The Surface Properties of Silicas*. (New York: Wiley, 1998).
5. FAO/WHO Codex Alimentarius Commission List of Additives Evaluated for their Safety-in-Use in Food CAC/Fal 1-1973.
6. Krupskaya T.V., Gun'ko V.M., Protsak I.S., Kartel M.T., Turov V.V. Control of the thixotropic properties of aqueous suspensions containing hydrophilic and hydrophobic components. *Him. Fiz. Tehnol. Poverhni*. 2020. **11**(1): 38.

7. Gun'ko V.M., Turov V.V., Pakhlov E.V., Matkovsky E.M., Krupskaya T.V., Kartel M.T., Charmas B. Blends of amorphous/crystalline and hydrophobic amorphous nanosilica. *J. Non-Cryst. Solids*. 2018. **500**: 351. [in Russian].
8. Gun'ko V.M., Turov V.V., Pakhlov E.V., Krupskaya T.V., Charmas B. Effect of water content on the characteristics of Hydro-compacted nanosilica. *Appl. Surf. Sci.* 2018. **459**: 171.
9. Turov V.V., Gun'ko V.M., Pakhlov E.V., Krupskaya T.V., Tsapko M.D., Charmas B., Kartel M.T. Influence of hydrophobic nanosilica and hydrophobic medium on water in hydrophilic components of complex systems. *Colloids Surf., A*. 2018. **552**: 39.
10. Somasundaran P. *Encyclopedia of Surface and Colloid Science, Third Edition*. (Boca Raton: Taylor & Francis, CRC Press, 2015).
11. Gun'ko V.M., Pakhlov E.M., Goncharuk O.V., Andriyko L.S., Marynin A.I., Ukrainets A.I., Charmas B., Skubiszewska-Zięba J., Blitz J.P. Influence of hydrophobization of fumed oxides on interactions with polar and nonpolar adsorbates. *Appl. Surf. Sci.* 2017. **423**: 855.
12. Gun'ko V.M., Turov V.V., Protsak I.S., Krupskaya T.V., Pakhlov E.M., Zhang D. Interfacial phenomena in composites with nanostructured succinic acid bound to hydrophilic and hydrophobic nanosilicas. *Colloid Interface Sci. Commun.* 2020. **35**: 100251.
13. Gun'ko V.M., Turov V.V., Pakhlov E.M., Krupskaya T.V., Borysenko M.V., Kartel M.T., Charmas B. Water Interactions with Hydrophobic versus Hydrophilic Nanosilica. *Langmuir*. 2018. **34**(40): 12145.
14. Gun'ko V.M., Turov V.V., Goncharuk O.V., Pakhlov E.M., Matkovsky O.K. Interfacial phenomena at a surface of individual and complex fumed nanooxides. *Surface*. 2019. **11**(26): 3.
15. Patent UA 138023. Krupskaya T.V., Turov V.V., Gun'ko V.M., Kartel M.T. Method of transferring a mixture of hydrophilic and hydrophobic silica into an aqueous medium by using high mechanical loads. 2019.
16. Patent UA 138129. Krupskaya T.V., Turov V.V., Kartel M.T. A method of converting hydrophobic silica into an aqueous medium by using high mechanical loads. 2019.
17. Kirsanov E.A., Matveenko V.N. *Non-Newtonian behavior of structured systems*. (Moscow: TECHNOSPHERE, 2016). [in Russian].
18. Nguyen C., Desgranges F., Roy G., Galanis N., Mare T., Boucher S., Anguemintsa H. Temperature and particle-size dependent viscosity data for water-based nanofluids – hysteresis phenomenon. *Int. J. Heat Fluid Flow*. 2007. **28**(6): 1492.
19. Cheng N.S., Law A.W.K. Exponential formula for computing effective viscosity. *Powder Technol.* 2003. **129**(1–3): 156.
20. Mahbubul I.M., Saidur R., Amalina M.A. Latest developments on the viscosity of nanofluids. *Int. J. Heat Mass Transfer*. 2012. **55**(4): 874.
21. Masuda H., Ebata A., Teramae K., Hishinuma N. Alteration of thermal conductivity and viscosity of liquid by dispersing ultra-fine particles (dispersion of  $\text{-Al}_2\text{O}_3$ ,  $\text{SiO}_2$  and  $\text{TiO}_2$  ultra-fine particles). *Netsu Bussei*. 1993. **7**(4): 227.
22. Humplik T., Lee J., O'Hern S.C., Fellman B.A., Baig M.A., Hassan S.F., Atieh M.A., Rahman F., Laoui T., Karnik R., Wang. E.N. Nanostructured materials for water desalination. *Nanotechnology*. 2011. **22**(29): 292001.
23. Yamaguchi Y., Yasutake N., Nagaoka M. Theoretical Prediction of Proton Chemical Shift in Supercritical Water Using Gas-Phase Approximation. *Chem. Phys. Lett.* 2001. **340**(1–2): 129.
24. Schneider W.G., Bernstein H.J., Pople J.A. Proton Magnetic Resonance Chemical Shift of Free (Gaseous) and Associated (Liquid) Hydride Molecules. *J. Chem. Phys.* 1958. **28**(4): 600.
25. Kinney D.R., Chaung I-S., Maciel G.E. Water and the Silica Surface As Studied by Variable Temperature High Resolution  $^1\text{H}$  NMR. *J. Am. Chem. Soc.* 1993. **115**(15): 6786.
26. Hindman J.S. Proton Resonance Chemical Shifts of Water in Gas and Liquid State. *J. Chem. Phys.* 1966. **44**(12): 4582.
27. Hindman J.C. Nuclear Magnetic Resonance Effects in Aqueous Solutions of 1-1 Electrolytes. *J. Chem. Phys.* 1962. **36**(4): 1000.
28. Buckingham A.D., Schaefer T., Schneider W.G. Solvent Effects in Nuclear Magnetic Resonance Spectra. *J. Chem. Phys.* 1960. **32**(4): 1227.
29. Mihean C., Ziskind M., Chazallon B., Focsa C., Destombes J.L. Formation of Large Water Clusters by IR Laser Resonant Desorption of Ice. *Appl. Surf. Sci.* 2005. **248**(1–4): 238.
30. Chaplin M. *Water Structure and Behavior*. <http://www.lsbu.ac.uk/water/>
31. Wiggins P.M. High and Low density Intracellular Water. *Coll. Mol. Biol.* 2001. **47**(5): 735.
32. Gun'ko V.M., Turov V.V. Structure of Hydrogen Bonds and  $^1\text{H}$  NMR Spectra of Water at the Interface of Oxides. *Langmuir*. 1999 **15**(19): 6405.
33. Turov V.V., Gun'ko V.M. *Clustered water and ways to use it*. (Kyiv: Naukova Dumka, 2011). [in Russian].

34. Glushko V.P. *Thermodynamic Properties of Individual Substances*. (Moscow: Science, 1978).
35. Gun'ko V.M., Turov V.V., Gorbik P.P. *Water at the interface*. (Kyiv: Naukova Dumka, 2009). [in Russian].
36. Gun'ko V.M., Turov V.V. *Nuclear Magnetic Resonance Studies of Interfacial Phenomena*. (New York: Taylor & Francis, 2013).
37. Gun'ko V.M., Turov V.V., Bogatyrev V.M., Zarko V.I., Leboda R., Goncharuk E.V., Novza A.A., Turov A.V., Chuiko A.A. Unusual Properties of Water at Hydrophilic/Hydrophobic Interfaces. *Adv. Colloid Interface Sci.* 2005. **118**(1–3): 125.
38. Aksnes D.W., Førland K., Kintys L. Pore size distribution in mesoporous materials as studied by <sup>1</sup>H NMR. *Phys. Chem. Chem. Phys.* 2001. **3**: 3203.
39. Petrov O.V., Furó I. NMR cryoporometry: Principles, applications and potential. *Prog. Nucl. Magn. Reson. Spectrosc.* 2009. **54**(2): 97.

*Received 24.07.2020, accepted 25.11.2020*